Microwave Performance of an Optically Controlled AlGaAs/GaAs High Electron Mobility Transistor and GaAs MESFET

RAINEE N. SIMONS, MEMBER, IEEE

Abstract—**This paper presents for the first time extensive experimental results which show the light-induced voltage, the increase in the drain current, the RF gain, and the change in the microwave scattering parameters of an AlGaAs/GaAs high electron mobility transistor (HEMT) under optical illumination of photon energy equal to or greater than the semiconductor band gap. From the de-embedded device scattering parameters, the change in the small-signal, lumped-element equivalent circuit model is computed. These results are compared and contrasted with those of a GaAs MESFET. Lastly, three potential applications of an optically controlled AlGaAs/GaAs HEMT are demonstrated: microwave amplifier gain control, detection, and mixing with an optically coupled local oscillator signal. Preliminary experiments on the optical control of a monolithic GaAs distributed amplifier are also presented.**

Measurements on a HEMT show that the light-induced voltage is 0.57 V and the increase in the drain current is 5 mA under 1.7 mW optical power at 0.83 μm. Further, the increase in magnitude of S_{21} with illumination ranges from 0.5 to 2.0 dB as V_{g_1} takes discrete values between −0.5 and −0.95 V. However, the phase of S_{21} is insensitive to optical illumination. The HEMT as a photodetector has an external quantum efficiency greater than 500 percent and a dark noise current of 27 pA/$\sqrt{\text{Hz}}$. Lastly, computations show that the response speed of the HEMT to an intensity-modulated optical signal is on the order of 11 ps.

I. INTRODUCTION

FUTURE ACTIVE phased array antennas based on gallium arsenide (GaAs) microwave monolithic integrated circuit (MMIC) technology will have a transmit module and/or a receive module integrated with each element or small group of radiating elements. These MMIC circuits will require a phase-coherent reference signal for synchronizing the transmit module, a digital phase shifter setting commands for steering the beam or for multiple beam formation, a phase-coherent reference signal for phase locking the local oscillator in the receive module, and finally a manifold for the IF or video signal. The use of conventional waveguides and coaxial cables for coherent RF and digital command signal distribution from a central unit would make the array prohibitively large, heavy, and complex. One solution to the above problem is to use optical interconnect techniques based on optical fiber and semiconductor laser diode technologies. State-of-the-art semiconductor laser diodes are capable of being directly modulated at microwave frequencies. Hence, these laser diodes have the potential to provide direct optical control of microwave devices. Direct optical control can provide gain adjustability in amplifiers, phase shifting in phase shifters, and frequency tuning or locking in oscillators (see [1] and [2] and references therein). Another attractive feature is that the optical fiber technology can vastly reduce the size and complexity of the signal distribution network. These advanced phased array concepts are being actively pursued by NASA for use in future space communication systems. The following investigations have indicated the feasibility for direct optical control of microwave devices.

Several authors have investigated the effect of optical illumination on the dc characteristics [3], [4] and the microwave characteristics [5]–[7] of GaAs metal semiconductor field effect transistors (MESFET's). Their investigations suggest that the photo response is due to (a) the optically injected carriers, which increase the conductivity of the material between the source and the drain [3]; (b) the photo generated gate current causing a potential drop in the gate resistance, which in turn causes the change in the drain current via the transconductance of the MESFET [4]; and (c) changes in the MESFET equivalent circuit element values caused by a net gate voltage, which results when the photovoltaic voltage in the gate Schottky barrier region is superimposed on the gate bias supply applied through an external gate resistor [6]. However, with the advent of the AlGaAs/GaAs high electron mobility transistor (HEMT), it is possible to achieve much higher response speed than conventional high-speed GaAs MESFET's (see [8] and [9] and references therein). This is so because of the two-dimensional high mobility channel which exists at the heterostructure interface. Further, a recent analytical study by the author taking into consideration material properties showed that the heterostructures have a higher sensitivity to optical illumination. When this investigation was extended to microwave device structures, it was observed that the dc characteristics of an AlGaAs/GaAs HEMT are more sensitive to optical illumination of photon energy equal to or greater than the

Manuscript received April 7, 1987; revised August 6, 1987.

The author is with the NASA Lewis Research Center, Cleveland, OH 44135.

IEEE Log Number 8717242.

0018-9480/87/1200-1444$01.00 ©1987 IEEE

semiconductor band gap [10] than those of a GaAs MESFET.

This paper presents for the first time extensive experimental results which show the sensitivity to optical illumination, that is, the light-induced voltage and, as a consequence, the change in the drain to source current, the transconductance, the microwave scattering parameters, and the gain of an AlGaAs/GaAs HEMT. Further, from the de-embedded device scattering parameters, the changes in the lumped-element equivalent circuit model due to optical illumination are also computed. These results are compared and contrasted with those of the GaAs MESFET. Finally, three potential system applications of optically controlled AlGaAs/GaAs HEMT's, in amplifier gain control, high-frequency photo detection, and down-conversion or mixing with an optically coupled local oscillator signal, are demonstrated. Preliminary experiments on the optical control of a monolithic GaAs distributed amplifier are also presented.

II. Theoretical Background

When an AlGaAs/GaAs HEMT or a GaAs MESFET device is optically illuminated by photons of energy equal to or greater than the semiconductor band gap, free electron hole pairs are generated in their active layers. This process increases the concentration of the minority carriers, for example the holes in an n-type channel. This increase in hole concentration, Δp, is proportional to αd if $\alpha d \ll 1$. Mathematically, Δp is expressed as

$$\Delta p = \frac{\tau}{d}\left[\frac{P_{\text{opt}}\lambda}{hc}\right](1 - e^{-\alpha d}) \tag{1}$$

where h is Planck's constant, P_{opt} is the incident optical power per unit area, λ is the wavelength of the incident light, α is the optical absorption coefficient of the semiconductor, d is the thickness of the active layer, τ is the minority carrier lifetime, and c is the speed of light in vacuum.

The light-induced voltage, V_{lit}, at the Schottky gate as a consequence of the excess hole concentration is expressed as

$$V_{\text{lit}} = \frac{kT}{q}\ln\left(\frac{p + \Delta p}{p}\right) \tag{2}$$

where k is the Boltzmann constant, T is the temperature in degrees Kelvin, and q is the electronic charge. The variable p is the equilibrium minority carrier concentration in the active layer and is given by

$$p = \frac{n_i^2}{n} \tag{3}$$

where n_i is the intrinsic carrier concentration, and n is the carrier concentration.

The optical performance of the HEMT or the MESFET is also characterized by the responsivity R, which is expressed as

$$R = \frac{I_p}{P_{\text{opt}}} \tag{4}$$

where I_p is the drain current when the incident optical power is P_{opt}.

The quantum efficiency η is the number of electron–hole pairs generated per incident photon of energy hc/λ and is related to R as follows:

$$\eta = \frac{hcR}{\lambda q}. \tag{5}$$

III. Experimental Setup

A low-noise $Al_{0.3}Ga_{0.7}As$/GaAs HEMT (MPD-H503, Gould Inc.) with recessed pi-gate of length 0.5 μm and width 280 μm, a low-noise, low-power GaAs MESFET (DXL 0503A, Gould Inc.) with recessed pi-gate of length 0.3 μm and width 280 μm, and a medium-power GaAs MESFET (RPX 2322, Raytheon Co.) with T gate of length 0.5 μm and width 500 μm are used for investigation. The HEMT and the MESFET are fabricated using molecular-beam and vapor-phase epitaxial growth systems, respectively. For optical illumination, an AlGaAs/GaAs laser diode (SL-620 S, Ortel Corp.) with a fiber pigtail is used. The laser diode operated at a wavelength of 0.83 μm and is capable of being directly modulated at 6 GHz. The optical power emitted from the 50/125 μm multimode graded index optical fiber pigtail was measured using a calibrated digital power meter and a photosensor (815, Newport Corp.) to be about 1.7 mW. The tip of the fiber is held at a distance of 1 mm from the devices.

The AlGaAs/GaAs HEMT and the GaAs MESFET devices are mounted on a 3/8 by 3/8 in, 25 mil thick alumina carrier. The alumina carrier also accommodates a pair of 50 Ω coplanar waveguides (CPW), which serve as the signal input and output ports. The device gate and drain pads, and the source pad, are wire bonded to the CPW center strip conductors and ground plane, respectively, in the common source configuration. The carrier is then mounted in a test fixture which has two 3.5 mm coaxial connectors for external connection. The test fixture also has provision for ensuring repeatable pressure contact between the terminals of the CPW's on the carrier and the two 3.5 mm coaxial connectors on the fixture. The gate and the drain terminals of the devices are biased through two broad-band coaxial 50 Ω matched bias networks (HP 11612A, Hewlett Packard) which mate with the test fixture. The test fixture and the bias networks are capable of operation from 0.045 to 26.5 GHz. A CPW calibration kit consisting of a 50 Ω through, short circuit, offset, and an open circuit on similar alumina carriers are used for calibrating the HP8510 automatic network analyzer and de-embedding the device scattering parameters.

A block schematic of the entire experimental setup is shown in Fig. 1. The carriers, the calibration kit, and the test fixture (Design Techniques) are shown in Fig. 2.

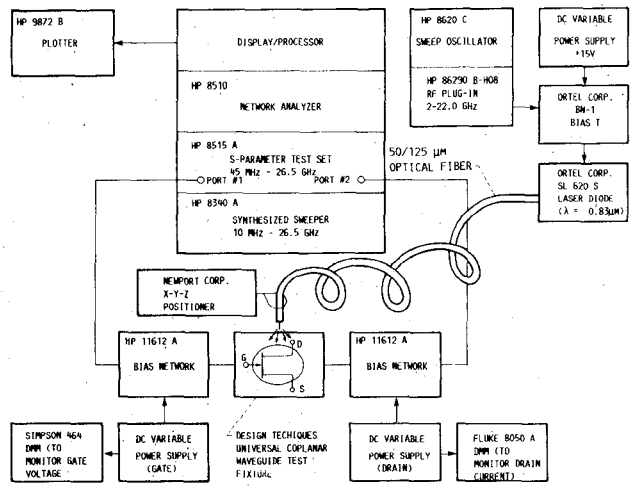

Fig. 1. Block schematic of the experimental setup.

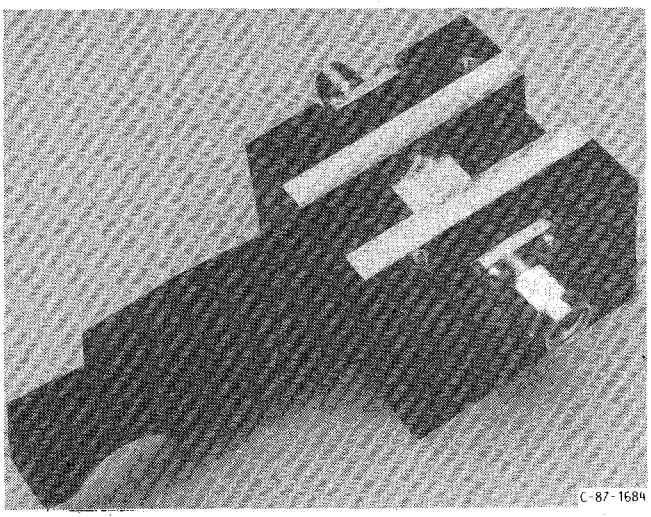

(a)

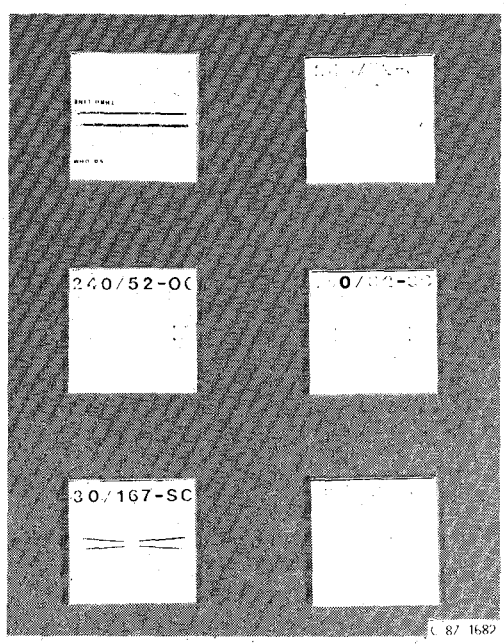

(b)

Fig. 2. (a) Design technique coplanar waveguide test fixture. (b) Design technique coplanar waveguide calibration kit.

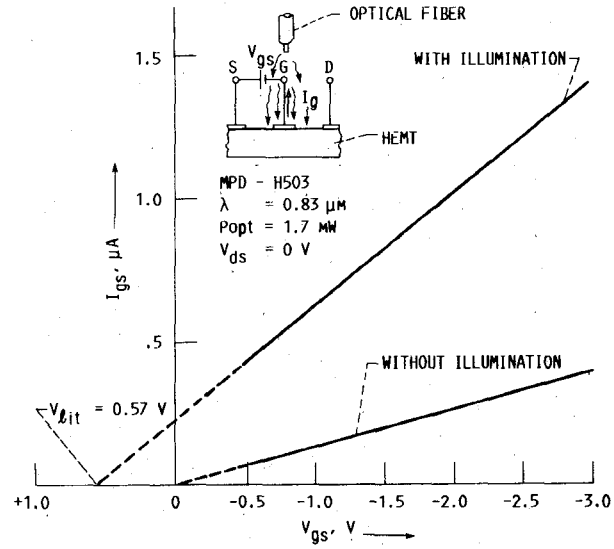

(a)

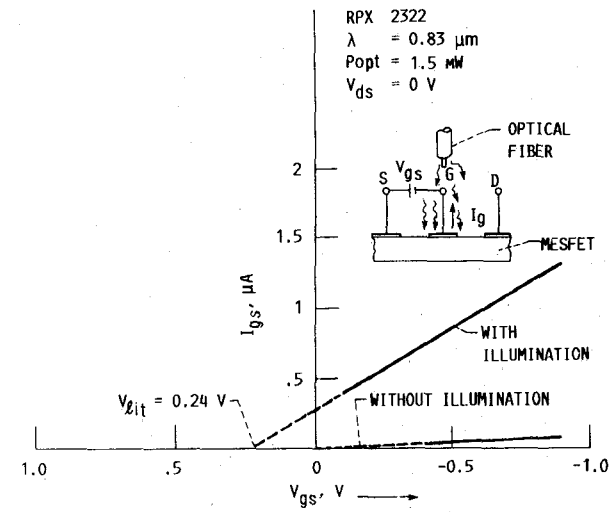

(b)

Fig. 3. (a) Measured I_g versus V_{gs} for AlGaAs/GaAs HEMT from which V_{lit} is obtained. (b) Measured I_g versus V_{gs} for GaAs MESFET from which V_{lit} is obtained.

IV. DC Device Characteristics under Optical Illumination

A. Light-Induced Voltage

Under optical illumination of photon energy equal to or greater than the GaAs semiconductor band gap, a photovoltaic effect appears at the Schottky gate of the AlGaAs/GaAs HEMT and GaAs MESFET. This photovoltage at the gate is termed the light-induced voltage, V_{lit}. V_{lit} is determined by plotting the measured gate current I_g as a function of the reversed biased gate-to-source voltage V_{gs}, with the drain open circuited, and extrapolating the curve till it intersects the abscissa. The intersection point is V_{lit}. Fig. 3(a) and (b) shows that V_{lit} is 0.57 and 0.24 V for the AlGaAs/GaAs HEMT and GaAs MESFET, respectively, when the optical illumination is approximately 1.7 mW. The higher value of V_{lit} for the AlGaAs/GaAs heterostructure is in accordance with theoretical predictions

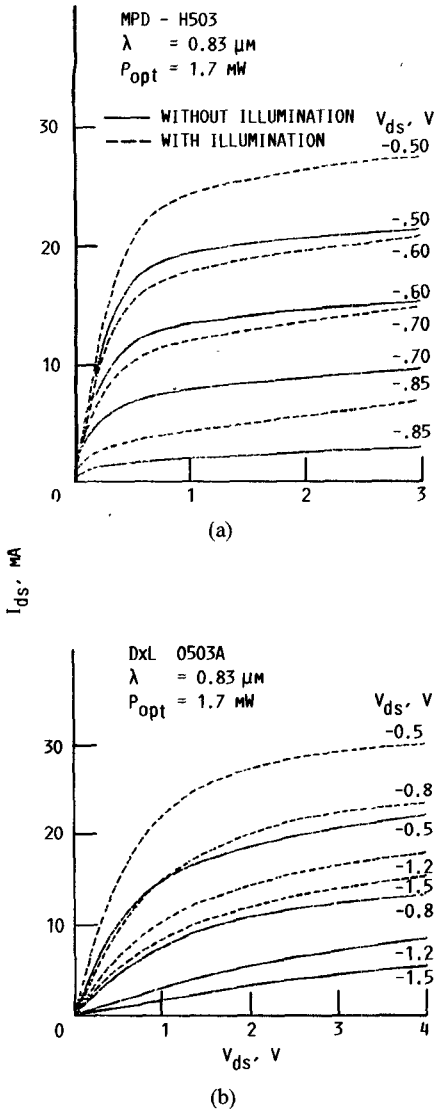

Fig. 4. (a) Measured I_{ds} versus V_{ds} for AlGaAs/GaAs HEMT with and without optical illumination. (b) Measured I_{ds} versus V_{ds} for GaAs MESFET with and without optical illumination.

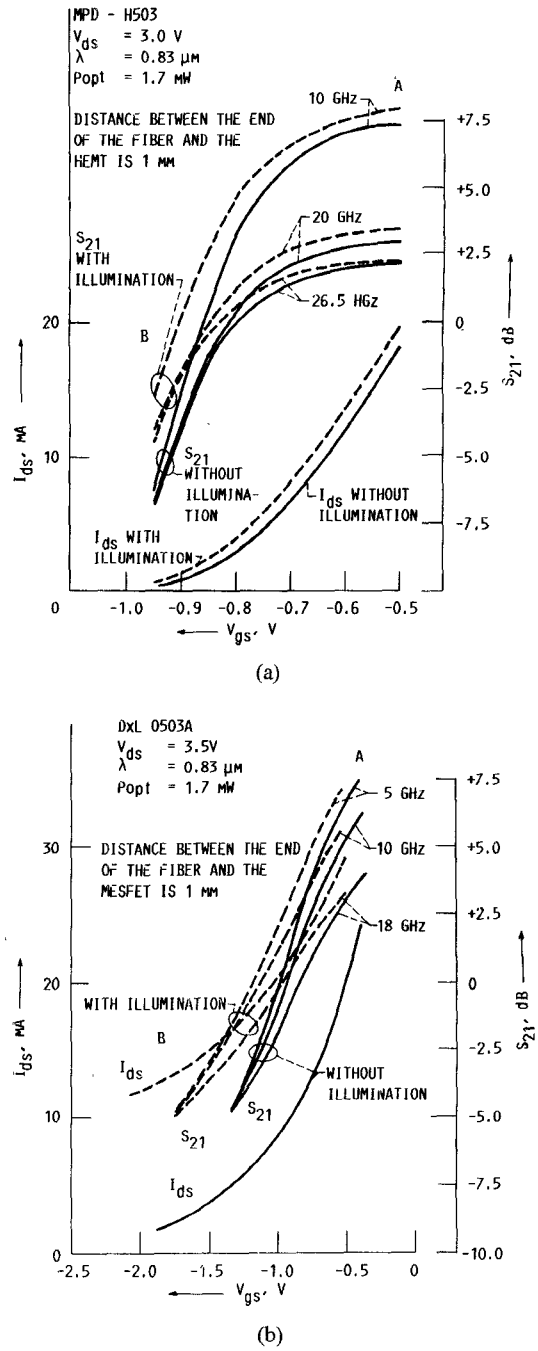

Fig. 5. (a) Measured gain versus V_{gs} for AlGaAs/GaAs HEMT with and without optical illumination. Point A is close to saturation and point B is close to pinchoff. (b) Measured gain versus V_{gs} for GaAs MESFET with and without optical illumination. Point A is close to saturation and point B is close to pinchoff.

[10]. Further, V_{lit} is independent of the gate-to-source and gate-to-drain spacings and is a function of the device material characteristics for a fixed incident optical power. In the above as well as in all the subsequent experiments, the gate is directly connected to a dc power supply without any external series resistor.

B. Drain Current versus the Drain-to-Source Voltage Characteristics

The measured drain-to-source current, I_{ds}, as a function of the drain-to-source voltage, V_{ds}, with and without optical illumination for an AlGaAs/GaAs HEMT and GaAs MESFET are presented in Fig. 4(a) and (b), respectively. This figure shows that the increase in the drain current at a fixed illumination for discrete values of V_{gs} is approximately 5.0 and 9.0 mA for the AlGaAs/GaAs HEMT and GaAs MESFET, respectively. The source-to-drain spacing for both devices is approximately 5 μm and the gate is centered between. Hence, the GaAs MESFET has a larger gate-to-source and also gate-to-drain spacing. The larger spacing increases the coupling efficiency between the incident radiation and the active layer and hence gives rise to more electron–hole pairs with a concomitant larger increase in drain current.

C. Transconductance

The measured dc transconductance, g_m, is observed to be insensitive to optical illumination. The maximum change observed with illumination is less than 2 mS.

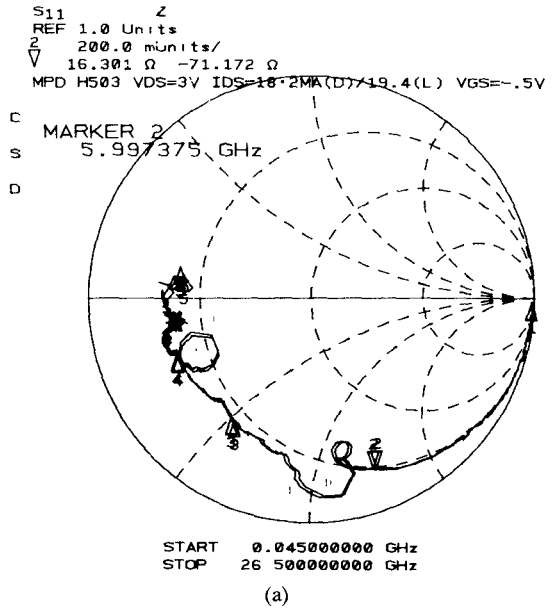

(a)

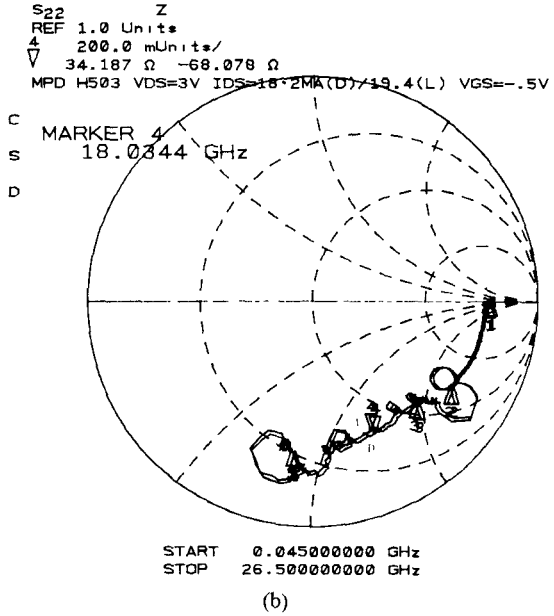

(b)

Fig. 6. Measured input and output reflection for AlGaAs/GaAs HEMT with and without optical illumination when biased at A. L denotes with illumination and D denotes without illumination. (a) S_{11}. (b) S_{22}.

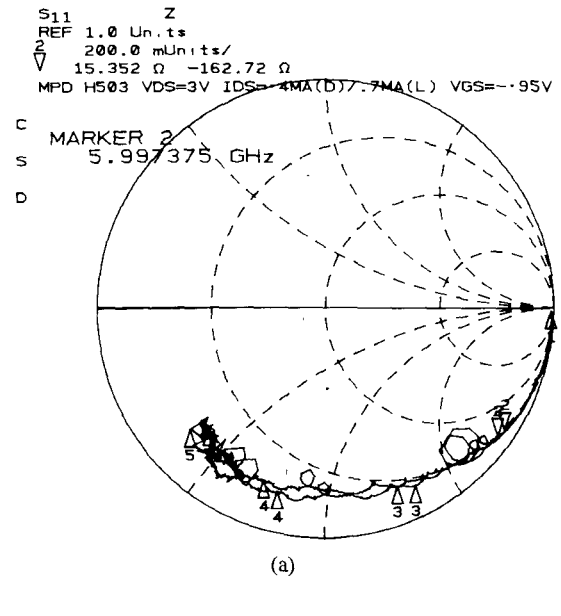

(a)

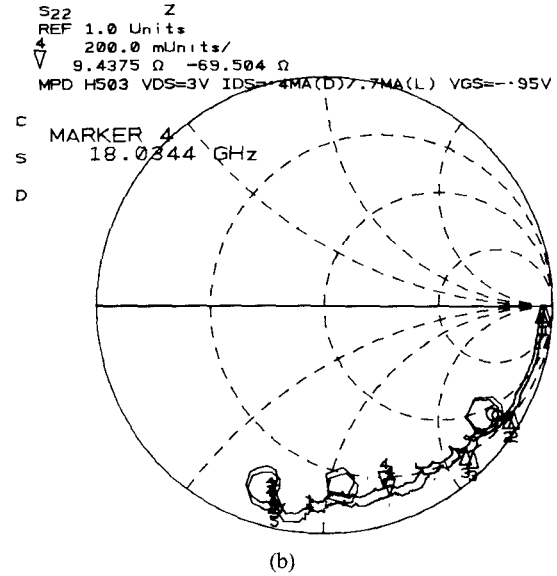

(b)

Fig. 7. Measured input and output reflection for AlGaAs/GaAs HEMT with and without optical illumination when biased at B. (a) S_{11}. (b) S_{22}.

V. Microwave Characteristics under Optical Illumination

A. Gain

The measured gain the test fixture with and without optical illumination as a function of V_{gs} for an AlGaAs/GaAs HEMT and a GaAs MESFET are presented in Fig. 5(a) and (b), respectively. This figure shows that the increase in gain is largest when the devices are biased close to pinchoff. As an example, for the case of an AlGaAs/GaAs HEMT, the gain increases by 2.5 dB at $V_{gs} = -0.95$ V and frequency equal to 26.5 GHz when the illumination is 1.7 mW.

B. Scattering Parameters

The HP8510 automatic network analyzer which is calibrated using the CPW calibration kit uses the through short, delay technique to de-embed the device scattering parameters and presents it as a function of the frequency. The scattering parameters, namely S_{11}, S_{22}, and S_{12}, are measured at a fixed drain bias with the gate bias taking several discrete values between saturation and pinchoff. However, in this section, the behavior of the device only when biased close to saturation and pinchoff will be presented. These bias points or operating points are labeled as point A and B, respectively, in Fig. 5(a) for the AlGaAs/GaAs HEMT and Fig. 5(b) for the GaAs MESFET.

The measured S_{11} over the frequency range 0.045 to 26.5 GHz for the AlGaAs/GaAs HEMT in saturation

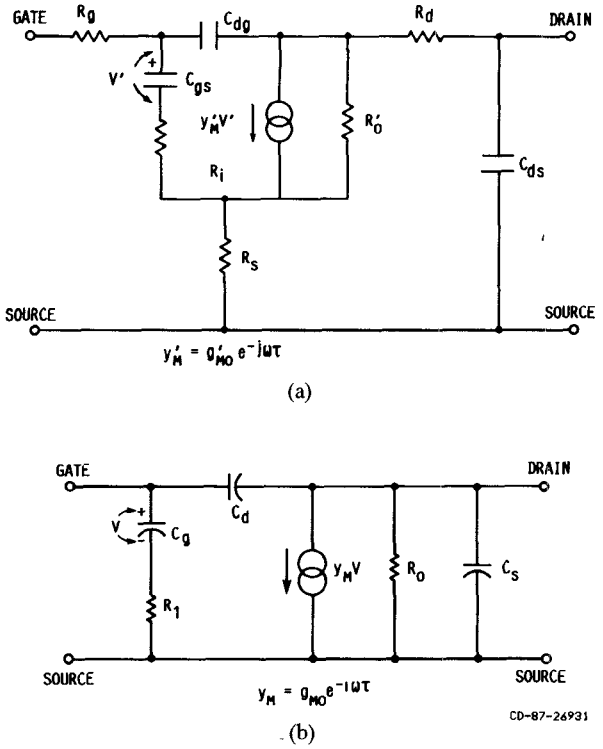

Fig. 8. (a) A lumped element equivalent circuit model for GaAs MESFET and AlGaAs/GaAs HEMT. (b) Pi equivalent circuit model due to Minasian.

($V_{gs} = -0.5$ V) and in pinchoff ($V_{gs} = -0.95$ V) conditions are illustrated on a Smith chart plot in Figs. 6(a) and 7(a), respectively. Similarly, S_{22} is illustrated in Figs. 6(b) and 7(b). In these figures, L and D denote that the measurements are carried out with or without optical illumination.

In the case of a GaAs MESFET, $V_{gs} = -0.3$ V and $V_{gs} = -1.4$ V corresponds to point A and B, respectively. S_{11}, S_{22}, and S_{12} were measured over the frequency range of 0.045 to 18.0 GHz. Thus from these measurements it is observed that optical illumination does affect S_{11}, S_{22}, and S_{12}; also, this effect is more pronounced when the devices are biased close to pinchoff.

C. Small-Signal, Lumped-Element Equivalent Circuit Model

The small-signal, lumped-element equivalent circuit model [11] for the AlGaAs/GaAs HEMT and GaAs MESFET operated in the saturated current region and in the common source configuration is shown in Fig. 8(a). The circuit elements R_s, R_d, R_g, C_{gs}, C_{dg}, and C_{ds} have their physical origin within the device and represent the source-to-channel resistance, drain-to-channel resistance, gate metal resistance, gate-to-channel depletion capacitance, drain-to-gate feedback capacitance, and drain-to-source capacitance, respectively. The circuit elements R_i, Y'_m, and R'_0 are associated with the Schottky barrier region and represent the charging channel resistance to C_{gs}, the transadmittance of magnitude g'_{m0} and phase delay τ (reflecting the carrier transit time in the channel section), and the channel resistance, respectively. Minasian [11] has shown that for a practical device $R_s/R'_0 \ll 1$ and $\mathrm{Re}\, Y'_{12}$

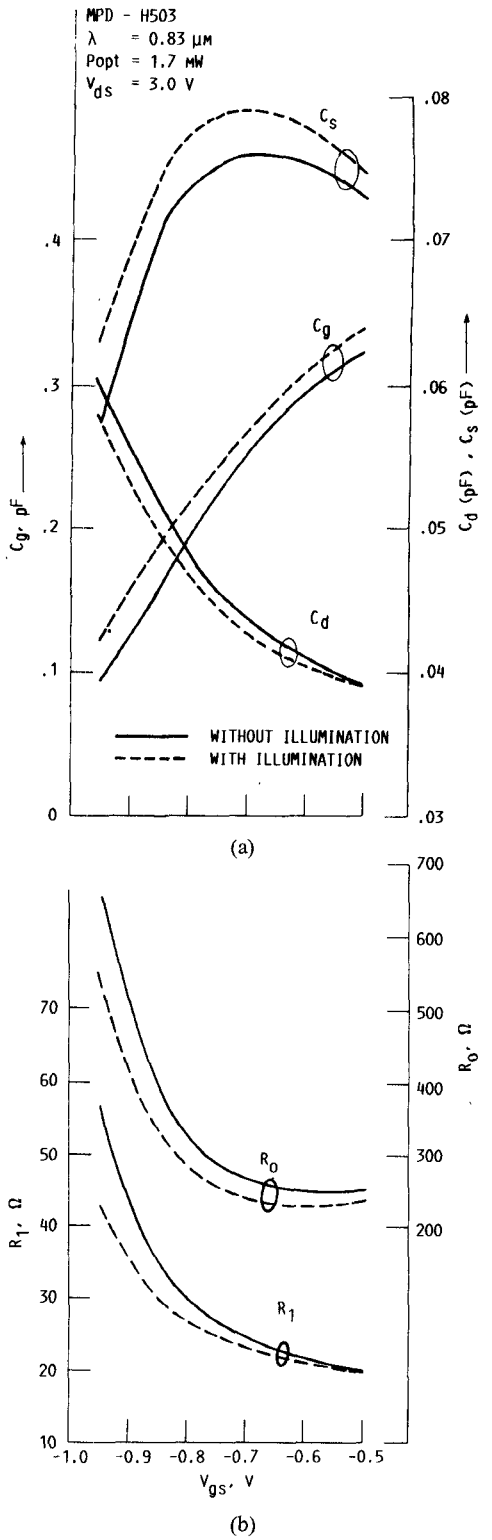

Fig. 9. De-embedded. (a) Gate, source, and drain-to-gate feedback capacitances. (b) Charging resistance and the channel resistance with and without optical illumination for AlGaAs/GaAs HEMT.

$\ll \mathrm{Im}\, Y'_{12}$. Hence without loss of accuracy the model of Fig. 8(a) can be transformed into a Pi equivalent model and is shown in Fig. 8(b). This model has been independently verified and found to be accurate up to 18 GHz [12]. The advantage of this model is that it is simple and conveniently related to the real and imaginary parts of the

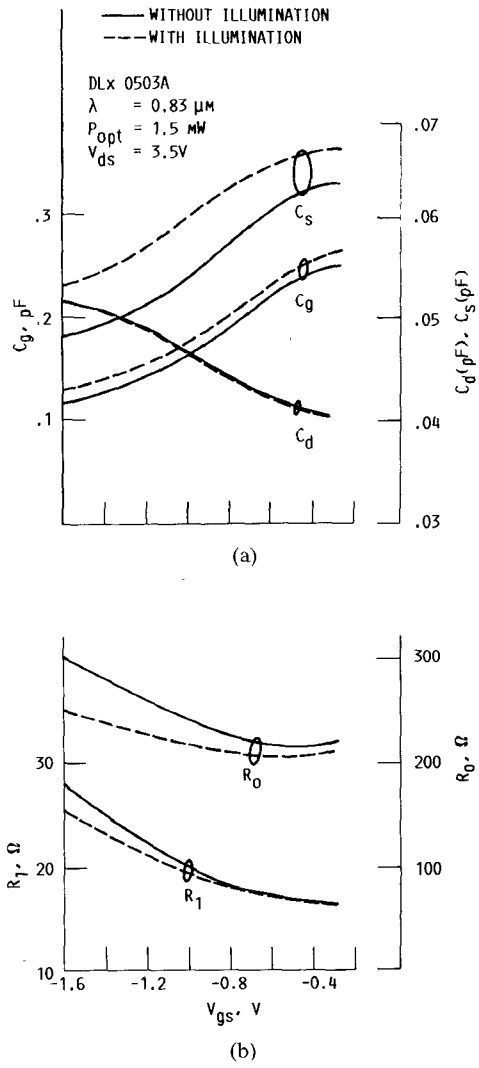

Fig. 10. De-embedded. (a) Gate, source, and drain-to-gate feedback capacitances. (b) Charging resistance and the channel resistance with and without optical illumination for GaAs MESFET.

admittance parameters. The expressions are [11]

$$C_d = -[\mathrm{Im}\, Y_{12}]/\omega$$
$$C_s = [\mathrm{Im}\, Y_{22}]/\omega - C_d$$
$$R_0 = 1/\mathrm{Re}\, Y_{22}$$
$$g_{m0} = \mathrm{Re}\, Y_{21} | \omega \to 0$$
$$C_g = [\mathrm{Im}\, Y_{11}]/\omega - C_d$$
$$R_1 = [\mathrm{Re}\, Y_{11}](\omega C_g)^2$$
$$\tau = \left(-[\mathrm{Im}\, Y_{21}]/\omega - g_{m0} R_1 C_g - C_d\right)/g_{m0}. \quad (6)$$

By substituting the measured admittance parameters in the above expressions, the changes in the equivalent circuit element values are computed and illustrated as a function of the gate bias voltage in Figs. 9 and 10. These figures show that the gate and source capacitances increase while the drain-to-gate feedback capacitance decreases under optical illumination. The gate charging resistance and the channel resistance both decrease under optical illumination.

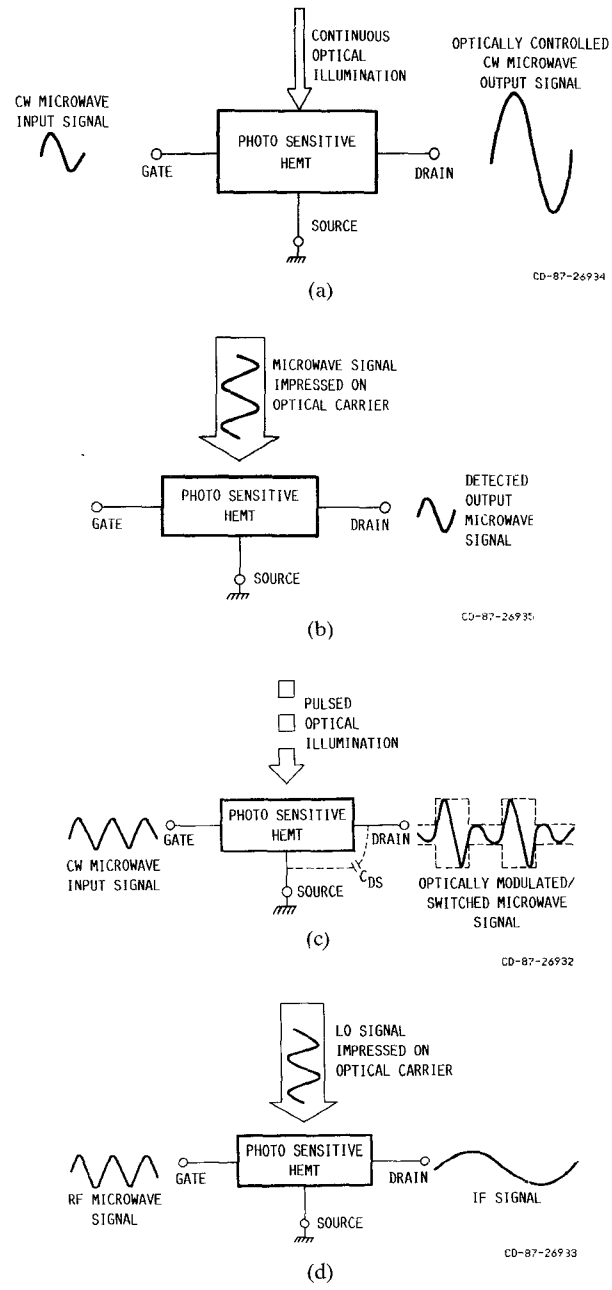

Fig. 11. Potential systems applications of an optically controlled AlGaAs/GaAs HEMT. (a) Optoelectronic microwave amplifier gain control. (b) Optoelectronic microwave detection. (c) Optoelectronic microwave modulation/switching. (d) Optoelectronic microwave mixing.

VI. Applications

Potential systems applications of an optically controlled AlGaAs/GaAs HEMT are schematically illustrated in Fig. 11.

A. Optoelectronic Microwave Amplifier Gain Control

The S_{21} of the HEMT device mounted in the test fixture is measured on the HP8510 Automatic Network Analyzer. Fig. 12(a) presents the magnitude of S_{21} without illumination as a function of the frequency for discrete values of V_{gs} varying between pinchoff and saturation. At this stage no attempt was made to match the drain and the

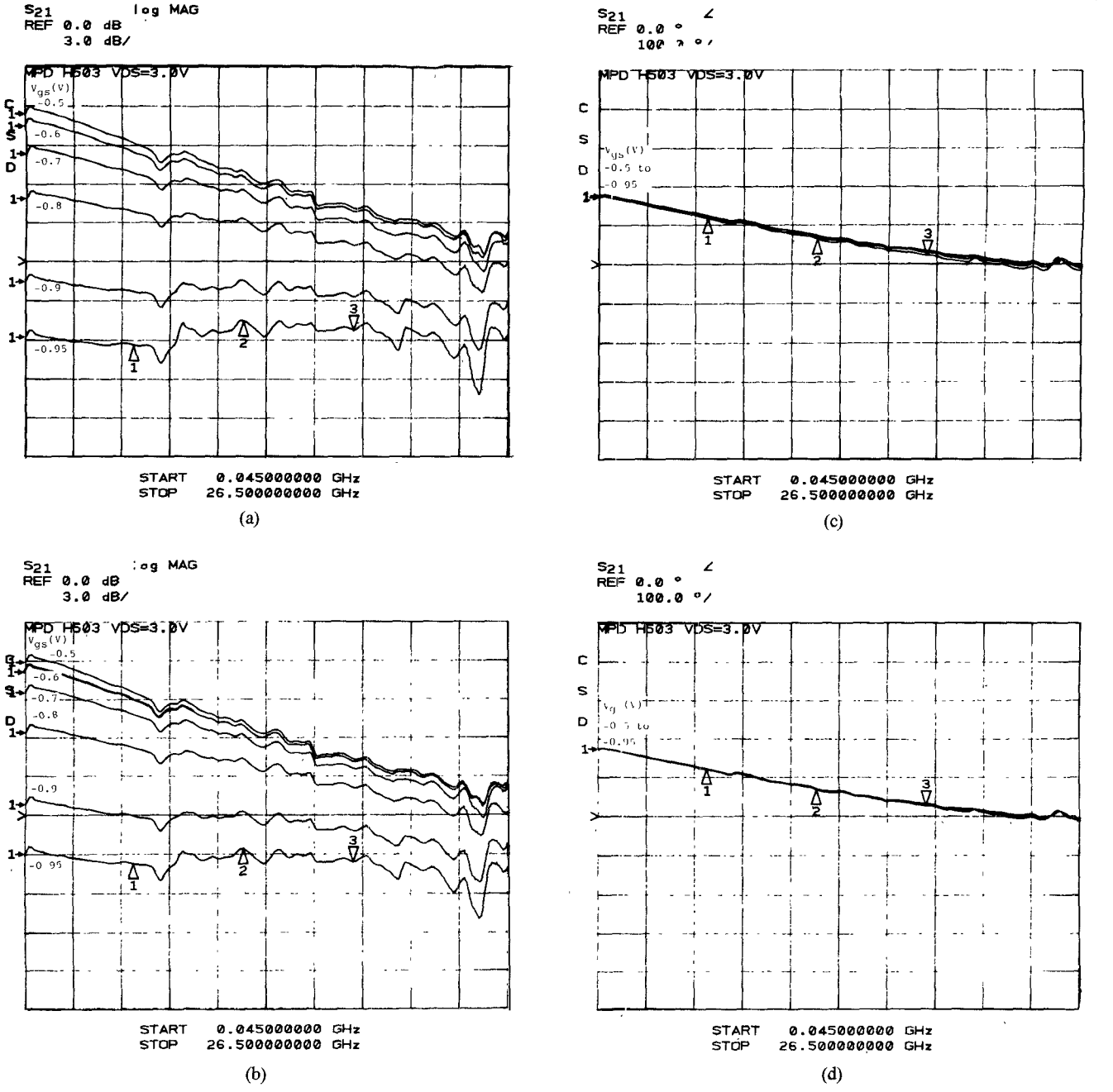

Fig. 12. Measured S_{21} for AlGaAs/GaAs HEMT. (a) S_{21} magnitude without optical illumination. (b) S_{21} magnitude with optical illumination. (c) S_{21} phase without optical illumination. (d) S_{21} phase with optical illumination.

gate input impedances. When the device is illuminated, the magnitude of S_{21} is observed to increase and the new set of characteristics are shown in Fig. 12(b). Comparing Fig. 12(a) with 12(b) at the center frequency of 13.25 GHz, the increase in the magnitude of S_{21} with illumination is observed to vary from 0.5 to 2.0 dB as V_{gs} takes discrete values between -0.5 and -0.95 V. On the other hand, from Fig. 13(a) and (b) for the GaAs MESFET at the center frequency of 9.0 GHz, the increase in the magnitude of S_{21} with illumination is observed to vary from 0.2 to 1.2 dB as V_{gs} takes discrete values between -0.3 and -1.6 V. Further, it is worth noting that the phase of S_{21} is insensitive to optical illumination, as is evident from Fig. 12(c) and (d) and Fig. 13(c) and (d). From a similar set of experiments it is observed that, if the optical illumination intensity is varied instead of V_{gs}, the magnitude of S_{21} can also be varied. The above experiments point toward a new technique of gain control in GaAs MMIC amplifiers.

In a third set of experiments, the GaAs MESFET chip used in the above experiments and a monolithic GaAs distributed amplifier chip were connected in a hybrid fashion. The distributed amplifier chip was developed by Texas Instruments Inc. [13] under a contract from NASA Lewis Research Center. The distributed amplifier is biased

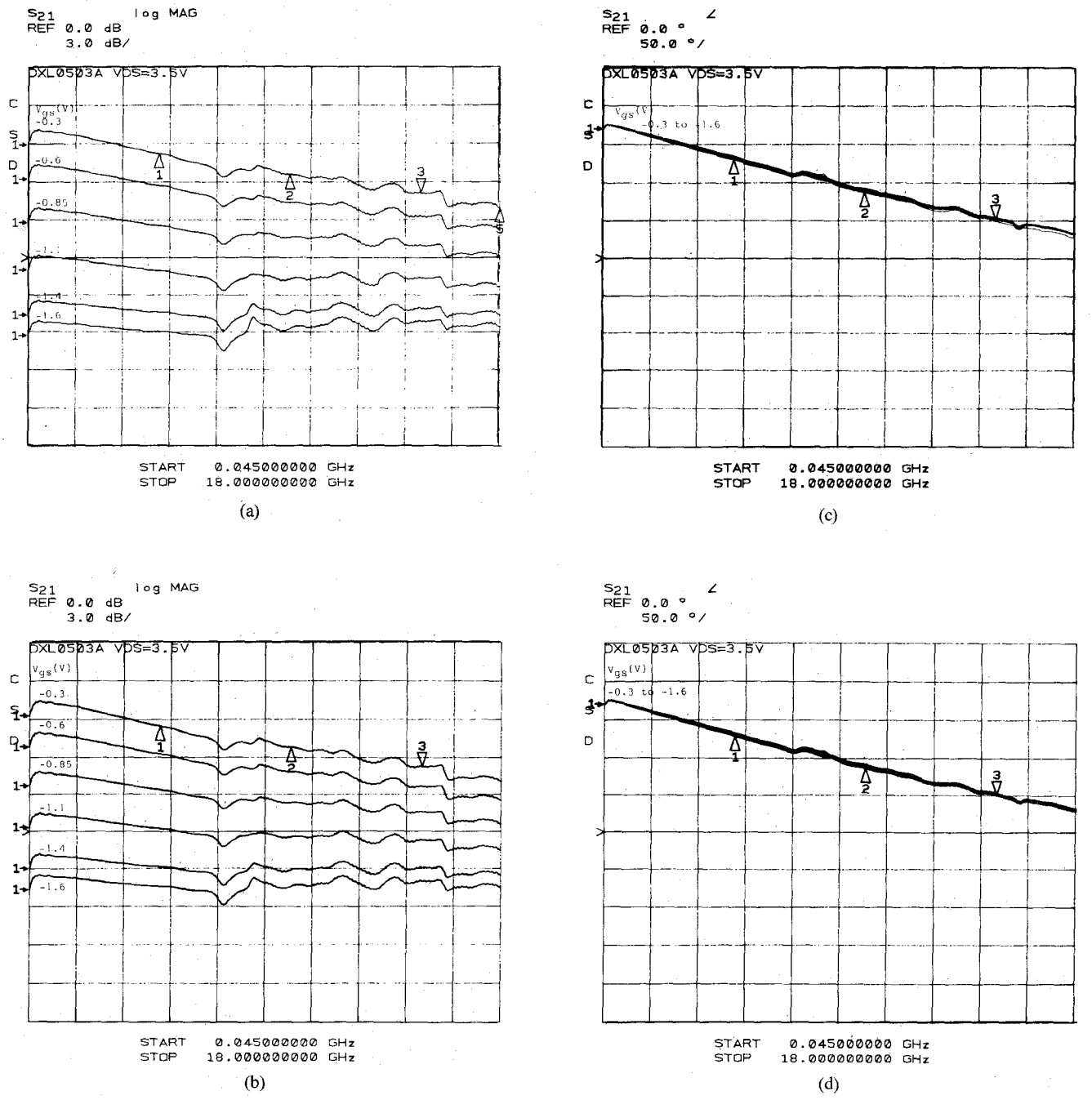

Fig. 13. Measured S_{21} for GaAs MESFET. (a) S_{21} magnitude without optical illumination. (b) S_{21} magnitude with optical illumination. (c) S_{21} phase without optical illumination. (d) S_{21} phase with optical illumination.

at $V_d = 6.3$ V and $V_g = -0.5$ V. The corresponding drain current I_d is 710 mA. The MESFET is biased such that $V_{ds} = 3.5$ V and $V_{gs} = -0.5$ V. The optical illumination on the MESFET is 1.5 mW. The drain current with and without optical illumination is 22 mA and 13 mA, respectively. The S_{21} of the hybrid circuit over the frequency range 2 to 18 GHz is observed to increase by 1 dB when the MESFET is illuminated. The experiment was repeated with V_{gs} set equal to -0.9 V and the observed increase in magnitude of S_{21} is almost 3 dB under illumination. These results are presented in Fig. 14(a) and (b), respectively.

B. Optoelectronic Microwave Detection and Optoelectronic Switching

Experiments were conducted by illuminating the AlGaAs/GaAs HEMT mounted in the test fixture with an optical signal of intensity 1.7 mW and modulated with a 6.0-GHz microwave signal. Further, the device is biased such that $V_{gs} = -0.5$ V and $V_{ds} = 3.0$ V. The HEMT under illumination showed a 6-mA increase in drain current. The detected 6.0-GHz signal as observed on a Spectrum Analyzer (HP 8566B, Hewlett Packard) is shown in Fig. 15(a).

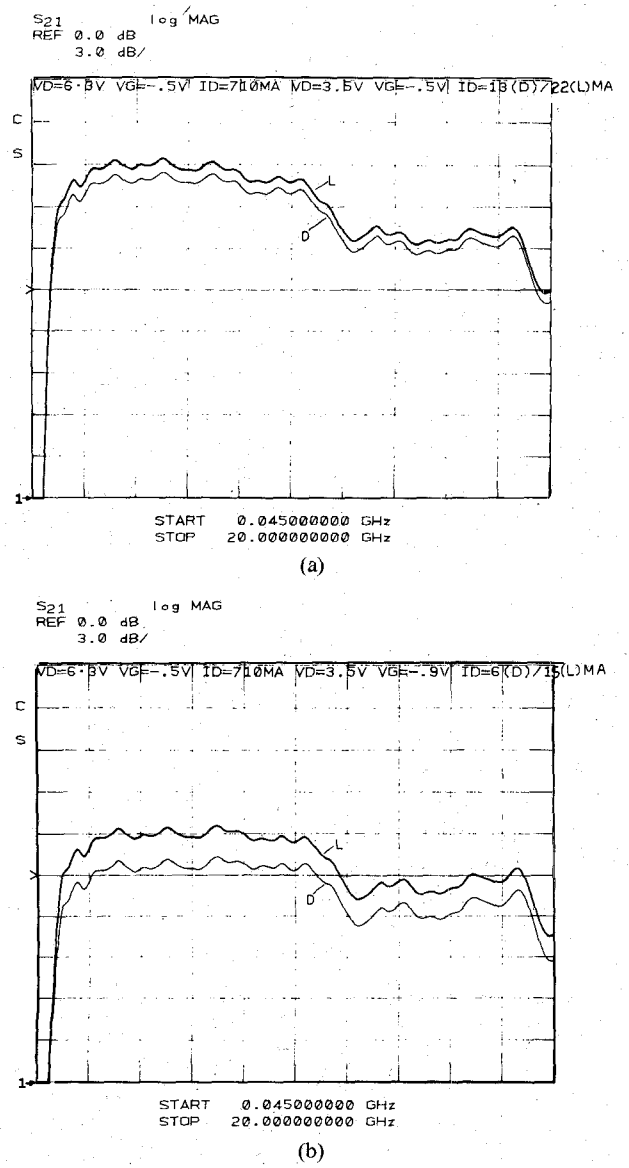

Fig. 14. Measured S_{21} magnitude of MESFET–FET distributed amplifier hybrid circuit with and without optical illumination. (a) When MESFET gate bias is -0.5 V. (b) When MESFET gate bias is -0.9 V.

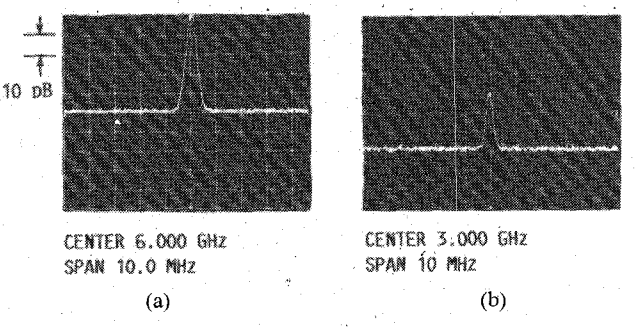

Fig. 15. (a) Detected 6-GHz signal. (b) 3-GHz IF signal.

The quantum efficiency of the AlGaAs/GaAs HEMT, when used as a photodetector, is estimated by comparing it with an AlGaAs/GaAs p-i-n photodiode (model PD 050-PM, Ortel Corp.) Light is coupled to the p-i-n photodiode also by a 50/125 μm fiber pigtail. The p-i-n photodiode has a responsivity of 0.35 A/W at 0.85-μm wavelength and a quantum efficiency of 50 percent [14]. Comparing the two devices, it is observed that the AlGaAs/GaAs HEMT with a responsivity of 3.53 A/W has an external quantum efficiency greater than 500 percent when $V_{gs} = -0.5$ V and $V_{ds} = 3.0$ V. In reality, the quantum efficiency is somewhat larger than this since the entire optical radiation from the end of the fiber does not impinge on the device active layer. This increase in optical gain is due to the generation of excess electron–hole pairs, which contributes to the increase in carriers in the conduction channel.

The noise spectrum of the AlGaAs/GaAs HEMT device without optical illumination is dominated by $1/f$ noise at frequencies below 100 MHz [15]; at high frequencies the channel conductance contributes to the noise, which is expressed as [16]

$$i_n^2 = 4kTg_mG\Delta f \tag{7}$$

where g_m is the transconductance of the AlGaAs/GaAs HEMT, Δf is the bandwidth, and G is a quantity approximately equal to 1.1 [17]. The computed noise current at room temperature and with a g_m of 40 turns out as 27 pA/$\sqrt{\text{Hz}}$.

The rise time of the AlGaAs/GaAs HEMT when illuminated by an intensity-modulated optical signal is estimated as follows. The HEMT device has an undoped GaAs layer of 1 μm thickness [18]. Assuming the velocity of the electrons to be 1.5×10^7 cm/s, the vertical transit time is 6.7 ps. Further, the electrons collected at the drain have to charge the small stray drain-to-source capacitance, C_{ds}, of 0.08 pF (from Fig. 9(a)), which results in a 2.2 RC time constant of 8.8 ps (assuming that the drain is terminated in 50 Ω resistance as in [4]). Thus the total response time is $((6.7+8.8)/\sqrt{2})$ approximately 11.0 ps. The factor $\sqrt{2}$ is responsible for converting the optical time constant to an electrical time constant [19]. Thus the response speed of the AlGaAs/GaAs HEMT to an intensity-modulated optical signal is on the order of 11 ps. In addition, the AlGaAs/GaAs HEMT has an f_t greater than 35 GHz and measurements indicate that the HEMT can provide useful gain at 26.5 GHz. Hence, as an approximation, if the upper 3-dB cutoff frequency is taken as 26.5 GHz and converted to rise time, a value of 13.2 ps results. This value is close to the response time obtained above taking the transit time and stray capacitance into account. It is worth noting that the response speed of the device is not influenced by C_g ($C_g \simeq 0.3$ pF from Fig. 9(a)) since C_g neither gets charged nor gets discharged during photodetection. Further, the gate is held at a fixed potential since it is directly connected to the bias supply.

C. Optoelectronic Microwave Mixing

Preliminary experiments with an AlGaAs/GaAs HEMT show that it is possible to optically couple a local oscillator signal. This is achieved by directly modulating the laser diode at the local oscillator frequency of 6 GHz. The laser diode output is made to illuminate the gate region of the device. The RF signal at 9 GHz is electrically coupled to

the gate terminal. The resulting IF signal at 3 GHz as observed on a Spectrum Analyzer is shown in Fig. 15(b). At this stage no attempt was made to integrate a bandpass filter for the RF signal at the gate or for the IF signal at the drain terminals.

VII. Conclusions and Discussions

The paper presents for the first time extensive experimental results which show the sensitivity to optical illumination of an AlGaAs/GaAs HEMT, that is, the light-induced voltage and as a consequence the change in the drain-to-source current, the transconductance, the gain, and the microwave scattering parameters. The light-induced voltage for the HEMT is observed to be 0.57 V, while for the GaAs MESFET it is 0.24 V when the optical illumination is 1.7 mW at a wavelength of 0.83 μm. Further, the increase in drain current with the above illumination for discrete V_{gs} is approximately 5.0 and 9.0 mA for the AlGaAs/GaAs HEMT and the GaAs MESFET, respectively. The light-induced voltage is independent of the gate-to-source and the gate-to-drain spacings and is a function of the material characteristics only at a fixed incident optical power per unit area. The GaAs MESFET shows a higher increase in drain current. This is so because of the larger spacings, which increase the coupling efficiency between the incident optical radiation and the active layer. The transconductance is observed to be insensitive to optical illumination. Experiments show that illumination does affect the scattering parameters and that this effect is more pronounced when the devices are biased close to pinchoff. Further, from the de-embedded device scattering parameters, the changes in the equivalent circuit element values due to optical illumination are computed. These computations show an increase in the gate and drain capacitance and a decrease in the gate charging and the channel resistances. The capacitance variation of the HEMT with optical illumination can be successfully exploited in the design of an injection locked oscillator.

Finally, three potential system applications of an optically controlled AlGaAs/GaAs HEMT, in amplifier gain control, microwave detection and down-conversion, or mixing with an optically coupled local oscillator signal, are demonstrated. The experiments on amplifier gain control show that at the center frequency of 13.25 GHz the increase in the magnitude of S_{21} (gain) with illumination is observed to vary from 0.5 to 2.0 dB as V_{gs} takes discrete values between -0.5 and -0.95 V. However, the phase of S_{21} is insensitive to optical illumination. Preliminary experiments on the optical control of a monolithic GaAs distributed amplifier are also presented. The HEMT, when used as a photodetector, has an external quantum efficiency greater than 500 percent at 0.83 μm. However, it may be possible to increase the quantum efficiency by an integrated fiber-optic coupler like the one discussed in [20]. Computations show that the high-frequency noise current is on the order of 27 pA/$\sqrt{\text{Hz}}$ at room temperature and also that the HEMT is capable of responding to an intensity-modulated optical signal with a rise time on the order of 11 ps. Another interesting application of the above HEMT device as a photodetector is in an optical interconnect. An optical interconnect for a future GaAs-based phased array will have a laser diode as a transmitter, an optical waveguide as a transmission medium, and a photodiode as a receiver [21]. The role of the photodiode is to detect intensity-modulated optical signals and convert them into electrical signals. These electrical signals are then amplified to the required digital electrical level for gain control and phase shifter setting. Besides, these electrical signals can also be used to subharmonically injection lock a free running oscillator such as a MESFET dielectric resonator oscillator. This technique has been successfully demonstrated in two excellent papers [22], [23] and is termed indirect optical injection locking or control.

In our experiments the HEMT is optically illuminated by an AlGaAs/GaAs laser diode. This feature further enhances the attractivness of the above experiments since it leads to the possibility of integrating a HEMT and a laser diode on a single MMIC chip to perform multiple circuit functions optically, such as switching, amplifier gain control, phase shifting, and mixing. Such an integration, when fully accomplished, not only promises improved MMIC circuit performance but also vastly simplifies the signal distribution and beam steering in future phased array antenna systems.

Acknowledgment

The author wishes to acknowledge R. Romanofsky of NASA Lewis Research Center and V. Sokolov of Honeywell Physical Sciences Center, Bloomington, for assistance in bonding the MESFET's and HEMT's used in the experiments and for technical discussions. The author also wishes to thank E. Haugland of NASA Lewis Research Center and P. Saunier of Texas Instruments Inc., Dallas, for technical discussions on MMIC distributed amplifiers.

References

[1] R. G. Hunsperger, "Optical control of microwave devices," in *Integrated Optical Circuit Engineering II*, SPIE vol. 578, S. Sriram, Ed. Bellingham: SPIE, pp. 40–45, Sept. 1985.

[2] J. Austin and J. R. Forrest, "Design concepts for active phased-array modules," *Proc. Inst. Elec. Eng.*, pt. F, vol. 127, pp. 290–300, Aug. 1980.

[3] J. C. Gammel and J. M. Ballantyne, "The OPFET: A new high speed optical detector," in *IEEE Int. Electron Devices Meeting Tech.* Dig., Dec. 1978, pp. 120–123.

[4] T. Sugeta and Y. Mizushima, "High speed photo response mechanism of a GaAs-MESFET," *Japan. J. Appl. Phys.*, vol 19, pp. L27–L29, Jan. 1980.

[5] H Mizuno, "Microwave characteristics of an optically controlled GaAs MESFET," *IEEE Trans. Microwave Theory Tech.*, vol. MTT-31, pp. 596–600, July 1983.

[6] A. A. A. DeSalles, "Optical control of GaAs MESFET's," *IEEE Trans. Microwave Theory Tech*, vol. MTT-31, pp. 812–820, Oct. 1983.

[7] J. L. Gautier, D. Pasquet, and P. Pouvil, "Optical effects on the static and dynamic characteristics of a GaAs MESFET," *IEEE Trans. Microwave Theory Tech*, vol. MTT-33, pp. 819–822, Sept. 1985.

[8] C. Y. Chen, A. Y. Cho, C. G. Bethea, P. A. Garbinski, Y. M. Pang, B. F. Levine, and K. Ogawa, "Ultrahigh speed modulation-doped heterostructure field-effect photodetectors," *Appl. Phys. Lett.*, vol. 42, pp. 1040–1042, June 1983.
[9] T. Umeda, Y. Cho, and A. Shibatomi, "Picosecond HEMT photodetector," *Japan. J. Appl. Phys.*, vol. 25, pp. L801–L803, Oct. 1986.
[10] R. N. Simons and K. B. Bhasin, "Analysis of optically controlled microwave/millimeter-wave device structures," *IEEE Trans. Microwave Theory Tech.*, vol. MTT-34, pp. 1349–1355, Dec. 1986.
[11] R. A. Minasian, "Simplified GaAs MESFET model to 10 GHz," *Electron, Lett.*, vol. 13, pp. 549–551, Sept. 1977.
[12] T. M. Reeder and W. B. Wylie, "CAD/CAM for GaAs IC's," in *Proc. Microwave Syst. Appl. Technol. Conf.*, Mar. 1983, pp. 461–474.
[13] B. Kim and H. Q. Tserng, "0.5 W, 2-21 GHz monolithic GaAs distributed amplifier," *Electron. Lett.*, vol. 20, pp. 288–289, Mar. 1984.
[14] Ortel Corporation Optoelectronic Products Catalogue.
[15] P. A. Folkes, "Characteristics and mechanism of $1/f$ noise in GaAs Schottky barrier field effect transistors," *Appl. Phys. Lett.*, vol. 48, pp. 344–346, Feb. 1986.
[16] A. Van der Ziel, *Noise, Sources, Characterization, and Measurements*. Englewood Cliffs, NJ: Prentice-Hall, 1970.
[17] W. Baechtold, "Noise behavior of GaAs field-effect transistors with short gate lengths," *IEEE Trans. Electron Devices*, vol. ED-19, pp. 674–680, May 1972.
[18] A. Swanson, J. Herb, and M. Yung, "First commercial HEMT challenges GaAs FETs," *Microwaves and RF*, vol. 24, pp. 107–118, Nov. 1985.
[19] G. Keiser, *Optical Fiber Communications*. New York: McGraw-Hill, 1983, p. 251.
[20] P. R. Prucnal, E. R. Fossum, and R. M. Osgood, "Integrated fiber-optic coupler for very large scale integration interconnects," *Opt. Lett.*, vol. 11, pp. 109–111, Feb. 1986.
[21] J. K. Carney, M. J. Helix, and R. M. Kolbas, "Gigabit opto-electronic transmitters," in *GaAs IC Symp. Dig.*, 1983, pp. 48–51.
[22] P. R. Herczfeld, A. S. Daryoush, V. M. Contarino, A. Rosen, Z. Turski, and A. P. S. Khanna, "Optically controlled microwave devices and circuits," in *1985 IEEE MTT-S Int. Microwave Symp. Dig.*, June 4–6, 1985, pp. 211–214.
[23] P. Wahi, Z. Turski, A. S. Daryoush, and P. R. Herczfeld, "Comparison of indirect optical injection locking techniques of multiple *X*-band Oscillators," in *1986 IEEE MTT-S Int. Microwave Symp. Dig.*, June 2–4, 1986, pp. 615–618.

✠

Rainee N. Simons (S'76–M'80) received the B.E. degree in electronics and communications from the Mysore University in 1972, the M.Tech. degree in electronics and communications from the Indian Institute of Technology, Kharagpur, in 1974, and the Ph.D. degree in electrical engineering from the Indian Institute of Technology, New Delhi, in 1983. His Ph.D. thesis investigated the propagation characteristics of slot line, coplanar waveguide and also finline at millimeter-wave frequencies.

He served as a lecturer in the Department of Electrical Engineering, R.V. College of Engineering, Bangalore, India, during the academic year 1974–75. In addition, he served as a Senior Scientific Officer-II/I in the Center for Applied Research in Electronics (CARE) at IIT New Delhi from 1979 to 1985. At CARE IIT New Delhi, he worked on millimeter-wave finline components and on toroidal latching ferrite phase shifters for phased arrays. Since 1985, he has been working as a Research Associate in the Solid State Technology Branch of the Lewis Research Center of the National Aeronautics and Space Administration (NASA) in Cleveland, OH. His current research interest is in the analysis and modeling of GaAs millimeter-wave semiconductor devices in MMIC's, direct optical control of MMIC modules in phased arrays, and superconductivity.

Dr. Simons held the post of IEEE Student Chapter Chairman at IIT New Delhi from 1978 to 1979. He also held the posts of IEEE India Council ED/MTT Society Chapter (New Delhi) Joint Secretary, Executive Committee Member, and Vice Chairman during the years 1982, 1983, and 1984, respectively.